Available online at www.sciencedirect.com

ScienceDirect

Ceramics International 35 (2009) 1611–1616

CERAMICS INTERNATIONAL

www.elsevier.com/locate/ceramint

Phase formation and dielectric properties of $(Pb,Ba)[(Zn_{1/2}W_{1/2}),Ti]O_3$ ceramics

Seung-Hyun Cho, Bong-Ho Lee, Nam-Kyoung Kim *

School of Materials Science and Engineering, Kyungpook National University, Daegu 702-701, Republic of Korea

Received 11 February 2008; received in revised form 9 July 2008; accepted 1 September 2008
Available online 30 September 2008

Abstract

$PbTiO_3$ and/or $BaTiO_3$ were systematically introduced into $Pb(Zn_{1/2}W_{1/2})O_3$ and resultant phase developments in terms of perovskite formation were investigated. Ceramic powders were prepared via a B-site precursor route to further assist the perovskite formation. Weak-field dielectric properties of the sintered samples were examined. For $Pb(Zn_{1/2}W_{1/2})O_3$-rich compositions, multiphase ceramics resulted and formation of monophasic perovskite turned out to be not successful even by the B-site precursor method. Values of the perovskite formation yield and the maximum dielectric constant increased with increasing fractions of the substituent species.

Keywords: A. Powders: Solid-state reaction; B. X-ray methods; C. Dielectric properties; D. Perovskites

1. Introduction

Lead magnesium tungstate $Pb(Mg_{1/2}W_{1/2})O_3$ (PMW) is a representative complex-perovskite antiferroelectric compound with a Curie temperature of 38 °C [1]. One interesting feature of PMW is the presence of extraneous superlattice peaks (in addition to the fundamental perovskite peaks) generated by macroscopic long-range 1:1 ordering between the octahedral cations of Mg^{2+} and W^{6+} [2,3], when examined by X-ray diffraction (XRD). To date, however, lead zinc tungstate $Pb(Zn_{1/2}W_{1/2})O_3$ (PZW, a zinc-analog of PMW) of a perovskite structure has not been synthesized. Phase developmental results on PbO + $(Zn_{1/2}W_{1/2})O_2$ could only be found [4], where mixed phases of Pb_2WO_5 and ZnO were only reported, instead of the desired perovskite. Compared with PMW, the inability in the perovskite formation in PZW can be attributed to the smaller electronegativity difference (END [5]) of 1.8 in Zn–O, whereas the value in Mg–O is 2.2. The inability can also be attributed to the somewhat larger size of Zn over Mg, ionic radii [6] of which are 0.0740 and 0.0720 nm, respectively.

Meanwhile, $PbTiO_3$ and $BaTiO_3$ (PT and BT, respectively) are representative perovskite compounds with well-known dielectric properties. They have also been reported to be highly effective in the perovskite stabilization in many $Pb(B',B'')O_3$ compositions, including $Pb(Zn_{1/3}Ta_{2/3})O_3$ [7] and $Pb(Zn_{1/3}Nb_{2/3})O_3$ [7–9]. In the present study, therefore, the two cation species of Ti and Ba were separately/simultaneously introduced into PZW to form $(Pb,Ba)[(Zn_{1/2}W_{1/2}),Ti]O_3$. The ionic radii [6] of Ti and Ba (0.0605 and 0.161 nm) are substantially smaller and larger than the respective host cation-complex/cations of $Zn_{1/2}W_{1/2}$ (0.067 nm, weight-averaged value) and Pb (0.149 nm). Consequently, the perovskite development in PZW may be induced by the compositional modification for increasing the geometrical tolerance factor and the END values as well.

Ceramic powders were prepared by a B-site precursor method [10,11], which is conceptually identical to (but a more comprehensive procedure than) the columbite process [12,13]. In the method, the $(B',B'')O_2$-type precursor powders were synthesized first and then reacted with the A-site component(s) to develop the perovskite structure. Therefore, the formation routes of unwanted pyrochlore(s) between Pb and the high-valence octahedral B″ cations (especially of Ta and Nb) could be fundamentally by-passed. The presence of parasitic pyrochlore (even in small quantities) has been reported to be quite detrimental to the dielectric properties, especially in the Pb-based complex-perovskite compositions [14–16].

---

* Corresponding author at: Kyungpook National University, School of Materials Science and Engineering 1370 Sankyuk-Dong, Buk-Gu, Daegu 702-701, Republic of Korea. Tel.: +82 53 950 5636; fax: +82 53 950 5645.
E-mail address: nkkim@knu.ac.kr (N.-K. Kim).

0272-8842/$34.00 © 2008 Elsevier Ltd and Techna Group S.r.l. All rights reserved.
doi:10.1016/j.ceramint.2008.09.004

2. Experimental

The investigated compositions were grouped as three systems of $(1-x)Pb(Zn_{1/2}W_{1/2})O_3$–$xPbTiO_3$, $(1-y)Pb(Zn_{1/2}W_{1/2})O_3$–$yBaTiO_3$, and $(1-z)Pb(Zn_{1/2}W_{1/2})O_3$–$z(Pb_{0.5}Ba_{0.5})TiO_3$ (PZW–xPT, PZW–yBT, and PZW–zP·BT in short, respectively) with the values of x, y, and z ranging from 0.0 to 1.0. Starting materials were high-purity chemicals of PbO (99.5%), $BaCO_3$ (99.9%), ZnO (99.8%), WO_3 (99.8%), and TiO_2 (99.9%). In order to maintain stoichiometries as closely to the nominal values as possible, the moisture contents of the raw materials and of the separately synthesized precursor powders were measured and introduced into the batch calculation.

As B-site compositions of the PZW–xPT, PZW–yBT, and PZW–zP·BT systems are identical as $(1-x)(Zn_{1/2}W_{1/2})O_2$–$xTiO_2$, precursor powders for the three systems were prepared simultaneously from constituent chemicals, except for $x = 1.0$ of TiO_2. The precursor batches were milled for 12 h under alcohol (ZrO_2 media, polyethylene container), dried overnight, and reacted at 650 °C for 2 h in air. The calcined powders were wet-milled, dried, and reacted for additional 2 h at identical temperatures in order to promote phase development. After identification of the developed phases in the precursor powders by X-ray diffractometry, required amounts of PbO and $BaCO_3$ were added. The batches were wet-milled, dried, and calcined first at 750–850 °C and then at 750–1150 °C (depending on composition) for 2 h each with intermediate milling/drying stages. The powders were also examined by XRD for phase identification.

An aqueous solution (2 wt.%) of a polyvinyl alcohol binder was added to the prepared powders and granulated, followed by uniaxial pressing to form pellet-type samples. The preforms were fired at 750–1350 °C for 1 h (soaking time) in a multiple-enclosure crucible setup (with atmospheric powders of identical composition surrounding the samples [17]) to minimize lead loss during exposure to high temperatures. Sintered specimens were ground/polished to attain parallel sides, onto which gold was sputtered as electrical contacts. Dielectric constant values of the ceramics were measured on cooling, using an impedance analyzer under weak-field (~1 V_{rms}/mm) low-frequency (1–1000 kHz) conditions.

3. Results and discussion

Phases developed in the B-site precursor $[(Zn_{1/2}W_{1/2})_{1-x}$-$Ti_x]O_2$ compositions are displayed in Fig. 1. The patterns of $x = 0.0$ and 1.0 were identified as wolframite ($ZnWO_4$, ICDD No. 15-774) and rutile (TiO_2, ICDD No. 21-1276), respectively, whereas the two phases coexisted at intermediate compositions. X-ray peaks of the starting materials were not detected at all (except for $x = 1.0$), confirming complete incorporation of the raw chemicals into the $(B',B'')O_2$-type precursor oxides. Meanwhile, parasitic peaks of anatase (TiO_2, ICDD No. 21-1272) were also detected whenever Ti was present ($x \geq 0.2$). It was reported, however, that the anatase phase was not observed whenever second components of $(Mg/Zn)(Ta/Nb)_2O_6$ were introduced to TiO_2 [7,18–20]. Therefore, the survival of anatase (even at $x < 1.0$) in the present study seems to be related to the presence of W component.

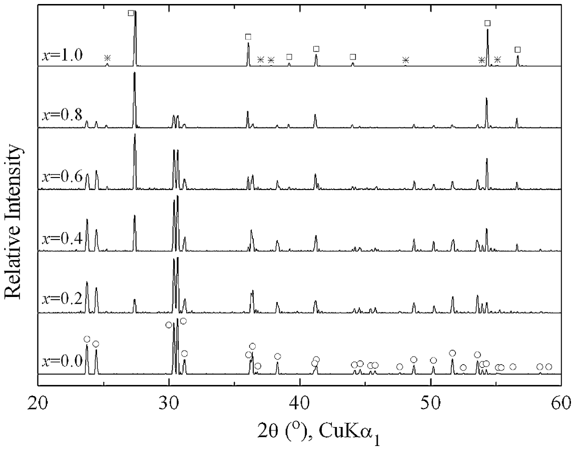

Fig. 1. XRD results of the B-site precursor $(1-x)(Zn_{1/2}W_{1/2})O_2$–$xTiO_2$. (○) wolframite, (□) rutile, and (*) anatase.

Relative fractions of the developed phases were estimated by comparing integrated intensities of the strongest peaks. Thus-obtained fractions of rutile + anatase are plotted in Fig. 2, along with the theoretical values. The experimentally determined results were virtually identical to the theoretical ones. Such an excellent agreement indicates that mutual solid solubilities between rutile/anatase and wolframite developed only limitedly (if at all) due presumably to the drastically different crystal structures.

X-ray diffraction results of the atmospheric powders (used during the sintering stage) in the three systems are contrasted in Fig. 3. At $x,y,z = 0.0$ (i.e., $Pb(Zn_{1/2}W_{1/2})O_3$), the major phase identified was Pb_2WO_5 (ICDD No. 36-1495, P_2W I hereinbelow) with small amounts of ZnO (ICDD No. 36-1451), as reported previously [4]. At $x = 0.2$ (PZW–xPT system, Fig. 3a), however, the P_2W I was replaced partly by another polymorph of Pb_2WO_5 (ICDD No. 37-306, P_2W II). At the same time, $Pb[(Zn_{1/2}W_{1/2}),Ti]O_3$ perovskite and $Pb_2Ti_2O_6$ pyrochlore (ICDD No. 26-142) phases also started to develop. At $x = 0.4$ and 0.6, intensities of the perovskite and pyrochlore increased further at the expense of P_2W I and II. The perovskite formation finally reached completion at $x = 0.8$, where the peaks of P_2W I, P_2W II, pyrochlore, as well as of ZnO disappeared completely.

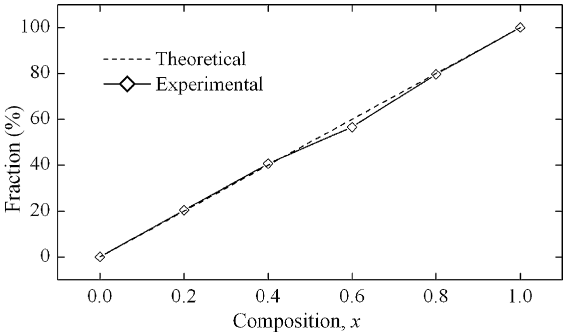

Fig. 2. Fractions of rutile + anatase in the precursor powder.

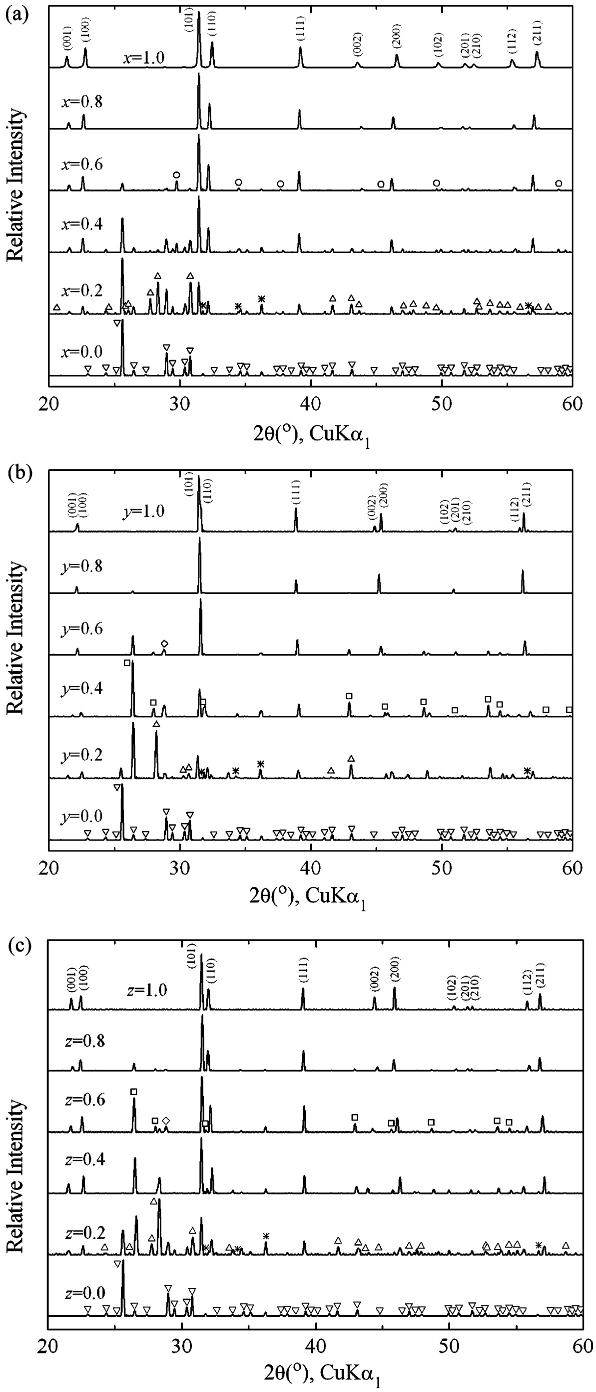

Fig. 3. Structure developments in (a) (1 − x)Pb($Zn_{1/2}W_{1/2}$)O_3–xPbTiO_3, (b) (1 − y)Pb($Zn_{1/2}W_{1/2}$)O_3–yBaTiO_3, and (c) (1 − z)Pb($Zn_{1/2}W_{1/2}$)O_3–z($Pb_{0.5}Ba_{0.5}$)-TiO_3. (▽) Pb_2WO_5 I, (△) Pb_2WO_5 II, (*) ZnO, (○) pyrochlore, (h k l) perovskite, (□) $BaWO_4$, and (◇) unknown.

In PZW–yBT (Fig. 3b) and PZW–zP·BT (Fig. 3c), the phase formation results were generally similar to that of the PZW–xPT system. However, a new compound of $BaWO_4$ (ICDD No. 43-646, BW) was identified at wide composition ranges of $0.2 \leq y,z \leq 0.8$, whereas the $Pb_2Ti_2O_6$ pyrochlore was not detected at all. The complete disappearance of the pyrochlore in the latter two systems seems to be associated with the presence of Ba (of much more ionic character than Pb [5]), which might have suppressed the pyrochlore formation by inducing perovskite development more readily. Meanwhile, the peaks (with substantial intensities) at $2\theta \approx 28.8^\circ$ ($0.2 \leq y \leq 0.6$ and $0.6 \leq z \leq 0.8$) could not still be identified satisfactorily. At first glance, a superlattice in the (Pb,Ba)[($Zn_{1/2}W_{1/2}$),Ti]O_3 perovskite seemed to be responsible for the peaks, similar to the superlattice peaks in Pb($Mg_{1/2}W_{1/2}$)O_3. By careful analysis, however, the possibility of superlattice development was excluded due to drastic mismatch in positions/intensities of the peak. Therefore, the peaks were left as 'unknown'.

Most of the peaks of a perovskite structure at $x,y,z = 1.0$ were obviously split, indicating non-cubic symmetries. The degrees of splitting, however, were not similar in the three systems, which resulted undoubtedly from different values of tetragonality (or axial ratio): $c/a = 1.065$ (PT, ICDD No. 6-452) and 1.011 (BT, ICDD No. 5-626). At intermediate compositions, separately formed [($Zn_{1/2}W_{1/2}$),Ti]O_2 precursors decomposed into ZnO, WO_3, and TiO_2, when reacted with PbO and/or $BaCO_3$ for perovskite formation. The latter two components then formed other tungstate compounds (Pb_2WO_5 and $BaWO_4$) and $Pb_2Ti_2O_6$ pyrochlore as well. On the contrary, the ZnO component was left unreacted and detected by X-ray diffraction, whenever the perovskite formation was incomplete ($x \leq 0.6$ and $y,z \leq 0.8$). Therefore, the B-site precursor method, which has been frequently adopted in the preparation of many Pb-based complex-perovskite compositions, turned out to be ineffective in the case of Pb($Zn_{1/2}W_{1/2}$)O_3.

Fractions of coexisting phases in the three systems were estimated from the XRD data (Fig. 3) and the results are presented in Fig. 4. In PZW–xPT (Fig. 4a), values of the perovskite increased continuously with increasing x at the expense of P_2W and ZnO. Fractions of the $Pb_2Ti_2O_6$ pyrochlore reached a maximum value (7.3%) at an intermediate composition of $x = 0.6$. The variations in PZW–yBT (Fig. 4b) and PZW–zP·BT (Fig. 4c) were basically similar to Fig. 4a. However, the pyrochlore phase present in the PZW–xPT system was replaced by an 'unknown' phase, whose fractions were also low (at most 9.6% and 4.9% at $y = 0.6$ and $z = 0.6$, respectively). Substantial amounts (as high as 50.2% ($y = 0.4$) and 27.4% ($z = 0.4$)) of BW were also developed at wide composition ranges of $0.2 \leq y,z \leq 0.8$. In PZW–yBT, fractions of BW were greatest among the three systems, whereas those of P_2W decreased most rapidly, both of which seem to be associated with the higher Ba concentration.

Phase development results of Pb($Zn_{1/3}B''_{2/3}$)O_3 (B″ = Nb or Ta) with PT and BT substitutions [7] are also included in Fig. 4 for comparison purposes. Pb($Zn_{1/3}Nb_{2/3}$)O_3 and Pb($Zn_{1/3}$-$Ta_{2/3}$)O_3 (PZN and PZTa, respectively) are well-known pyrochlore-prone compositions, perovskite formation of which by conventional solid-state reaction has not succeeded yet. Instead, perovskite powder of the former could only be prepared by applying high pressure [21] or mechanochemical milling [22], whereas synthesis of the latter by any means is still unreported. Between the two compositions, perovskite formation in PZN was achieved at substantially lower concentrations, regardless of PT and BT.

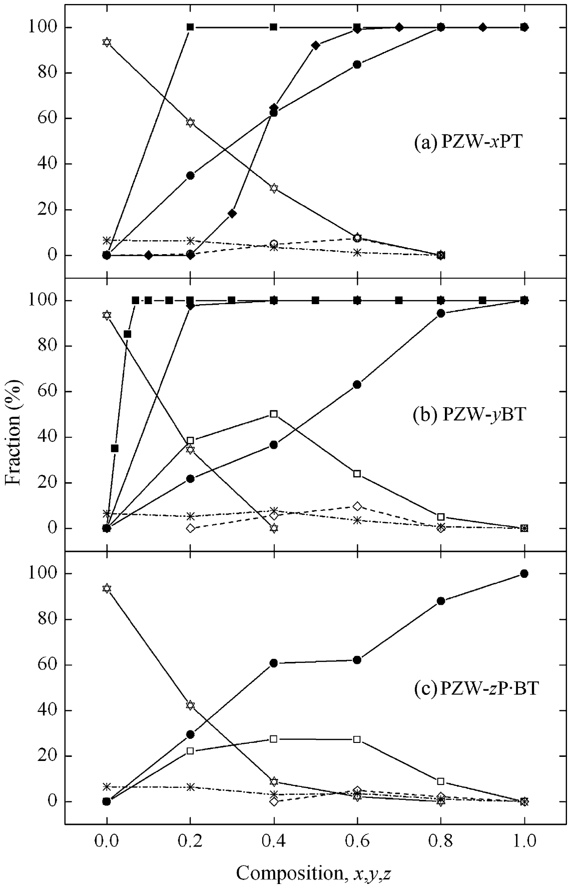

Fig. 4. Fractions of developed phases in the three systems: (✡) P_2W I + P_2W II, (*) ZnO, (○) pyrochlore, (●) perovskite, (□) $BaWO_4$, and (◇) unknown. Corresponding values of PZN/PZTa-PT and PZN/PZTa-BT are included in (a) and (b), respectively. (■) PZN and (◆) PZTa.

When the results are compared with those of PZW, PZN was the easiest for perovskite formation among the three host compositions. As for the two remaining compositions, perovskite formation in PZW was completed at much higher BT concentrations than in PZTa (Fig. 4b). When PT was used as a stabilizer (Fig. 4a), however, a perovskite phase in PZW started to develop earlier than in PZTa, whereas completion was achieved at lower substituent concentrations in PZTa.

Perovskite formation yields in the three systems (PZW–xPT, PZW–yBT, and PZW–zP·BT) are compared in Fig. 5, where the contents increased more or less continuously with increasing fractions of the substituent components. In addition, the effectiveness of PT as a perovskite stabilizer for PZW turned out to be somewhat higher than that of BT, whereas opposite trends were reported for PZN and PZTa (as discussed earlier). It is also noteworthy that the perovskite yields in PZW–zP·BT at low substituent fractions were closer to the values in PZW–xPT, whereas the contents at high fractions were closer to those in PZW–yBT. The strange behavior could be related to the different reaction capacity of Pb and Ba with Zn and/or W. Currently, it seems that Pb plays a more important role at low concentration range, whereas Ba deprives W from Pb to reduce the perovskite yield at high substitution level. Meanwhile, the powder compacts of $x,y,z = 0.0$ ($Pb(Zn_{1/2}W_{1/2})O_3$) could not be sintered properly. In addition, the sintered samples of $x = 1.0$ ($PbTiO_3$) and $z = 1.0$ ($(Pb_{0.5}Ba_{0.5})TiO_3$) were so brittle (due to microcrack developments during cooling by large structural anisotropy from high tetragonality) for further characterization that only the remaining compositions were examined for the rest of the study.

Dielectric constant values (1 MHz) of the ceramics in the three systems are shown in Fig. 6. Dependencies of the maximum dielectric constant and dielectric maximum temperature upon compositional change are plotted in Fig. 7. The dielectric constant values at $x,y,z \leq 0.4$ were very low (at most 540 at $x = 0.4$), which seems to be directly associated to the low perovskite contents. With increasing substituent fractions, maximum dielectric constant values increased continuously up to 7800 ($x = 0.8$) and 14,000 ($y = 1.0$). In addition, phase transition modes of the two compositions were very sharp with little dielectric dispersion of frequency dependence. At intermediate compositions, the spectra diffused with somewhat intermediate values of the maximum dielectric constant: 940

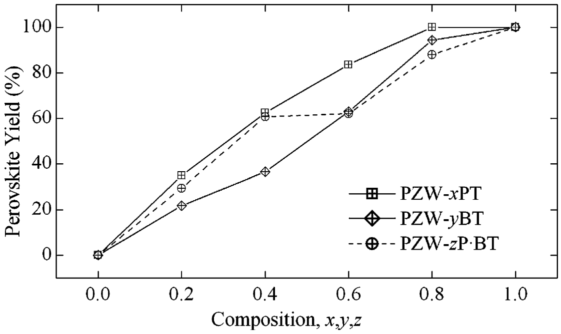

Fig. 5. Perovskite formation yields in the three systems.

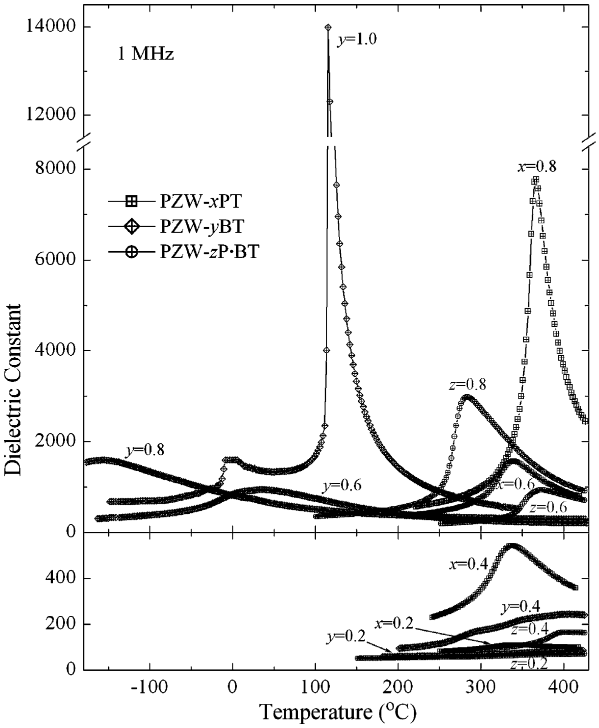

Fig. 6. Dielectric constant spectra of the ceramics.

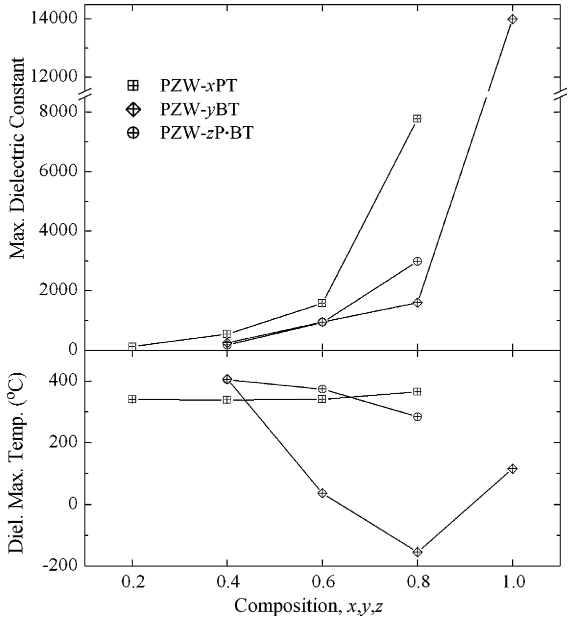

Fig. 7. Variation of maximum dielectric constant and corresponding temperature with compositional change.

($y,z = 0.6$) to 3000 ($z = 0.8$). Magnitudes of the dielectric maximum temperature (T_{max}) in PZW–*x*PT and PZW–*z*P·BT were 338–365 and 283–405 °C, rather insensitive to the compositional changes, when compared with a substantial decrease to as low as −155 °C ($y = 0.8$) in PZW–*y*BT, followed by an abrupt increase to 115 °C ($y = 1.0$). The reason why the dielectric maximum temperatures of certain compositions in PZW–*y*BT were so low is not clear at the moment and needs to be investigated further. By extrapolating T_{max} values at low substituent fractions, the T_{max} of PZW seems to be at least higher than those of BT and P·BT, but lower than that of PT. Actual T_{max} value of PZW can be determined only when perovskite phase is prepared.

4. Summary

In the B-site precursor compositions of $[(Zn_{1/2}W_{1/2}),Ti]O_2$, only the phases of wolframite and rutile (along with parasitic anatase) were detected, whose contents showed excellent agreement with the theoretical analysis. After the addition of PbO and/or $BaCO_3$ (followed by proper calcination), formation of monophasic perovskite was only observed when the molar fraction of PZW is ≤ 0.2. On the contrary, multiphase ceramics were obtained for higher PZW concentrations. Besides, the phase developed at $x,y,z = 0.0$ ($Pb(Zn_{1/2}W_{1/2})O_3$) was not perovskite, but Pb_2WO_5 and ZnO instead. Therefore, the B-site precursor method turned out to be ineffective in the synthesis of $Pb(Zn_{1/2}W_{1/2})O_3$ perovskite. With increase in the concentration of substituent species, the phase constitutions in the three systems became quite complicated, and $Pb_2Ti_2O_6$, $BaWO_4$, as well as another polymorphic form of Pb_2WO_5 were developed. The fractions of $BaWO_4$ were proportional to the Ba concentration, whereas the $Pb_2Ti_2O_6$ pyrochlore was only detected in the case of PZW–*x*PT. Nevertheless, the perovskite development yields increased continuously with increasing substituent fractions in all of the three systems. Meanwhile, the perovskite fractions in the PZW–*x*PT system were somewhat higher than those in the other two systems in the entire composition range.

The maximum dielectric constant values also increased with increasing substituent fractions in the three systems. The dielectric maximum temperatures in the PZW–*x*PT and PZW–*z*P·BT systems were comparatively insensitive to the compositional changes, whereas the variations in PZW–*y*BT were much larger in temperature. The T_{max} value of PZW seems to be higher than those of BT and P·BT, but lower than that of PT.

References

[1] L.A. Shuvalov, K.A. Minaeva, Anomalies of elasticity and internal friction in the region of the antiferroelectric Curie point of $PbMg_{1/2}W_{1/2}O_3$, Sov. Phys. -Dokl. 7 (1963) 906–907.

[2] A.I. Agranovskaya, Physical–chemical investigation of the formation of complex ferroelectrics with the perovskite structure, Bull. Acad. Sci. USSR Phys. Ser. 24 (1960) 1271–1277.

[3] V.A. Isupov, Causes of phase-transition broadening and the nature of dielectric polarization relaxation in some ferroelectrics, Sov. Phys. Solid State 5 (1963) 136–140.

[4] W.-J. Lee, N.-K. Kim, Phase developments in $Pb(Mg_{1/2}W_{1/2})O_3$ and $Pb(Zn_{1/2}W_{1/2})O_3$ via B-site precursor route, J. Mater. Sci. 43 (2008) 3608–3611.

[5] W.F. Smith, Principles of Materials Science and Engineering, 2nd ed., McGraw-Hill, Singapore, 1990, p. 37.

[6] R.D. Shannon, Revised effective ionic radii and systematic studies of interatomic distances in halides and chalcogenides, Acta Crystallogr. A 32 (1976) 751–767.

[7] J.-S. Kim, N.-K. Kim, H. Kim, Perovskite formation and dielectric characteristics of $Pb(Zn_{1/3}Ta_{2/3})O_3$ with $PbTiO_3$ substitution, J. Am. Ceram. Soc. 86 (2003) 929–933.

[8] J.R. Belsick, A. Halliyal, U. Kumar, R.E. Newnham, Phase relations and dielectric properties of ceramics in the system $Pb(Zn_{1/3}Nb_{2/3})O_3$–$SrTiO_3$–$PbTiO_3$, Am. Ceram. Soc. Bull. 66 (1987) 664–667.

[9] A. Halliyal, U. Kumar, R.E. Newnham, L.E. Cross, Stabilization of the perovskite phase and dielelctric properties of ceramics in the $Pb(Zn_{1/3}Nb_{2/3})O_3$–$BaTiO_3$ system, Am. Ceram. Soc. Bull. 66 (1987) 671–676.

[10] B.-H. Lee, N.-K. Kim, J.-J. Kim, S.-H. Cho, Perovskite formation sequence by B-site precursor method and dielectric properties of PFW-PFN ceramics, Ferroelectrics 211 (1998) 233–247.

[11] S. Ananta, N.W. Thomas, A modified two-stage mixed oxide synthetic route to lead magnesium niobate and lead iron niobate, J. Eur. Ceram. Soc. 19 (1999) 155–163.

[12] S.L. Swartz, T.R. Shrout, Fabrication of perovskite lead magnesium niobate, Mater. Res. Bull. 17 (1982) 1245–1250.

[13] S.L. Swartz, T.R. Shrout, W.A. Schulze, L.E. Cross, Dielectric properties of lead magnesium niobate ceramics, J. Am. Ceram. Soc. 67 (1984) 311–315.

[14] J. Chen, A. Gorton, H.M. Chan, M.P. Harmer, Effect of powder purity and second phases on the dielectric properties of lead magnesium niobate ceramics, J. Am. Ceram. Soc. 69 (1986) C303–C305.

[15] T.R. Shrout, A. Halliyal, Preparation of lead-based ferroelectric relaxors for capacitors, Am. Ceram. Soc. Bull. 66 (1987) 704–711.

[16] M.F. Yan, H.C. Ling, W.W. Rhodes, Preparation and properties of PbO–MgO–Nb_2O_5 ceramics near the $Pb(Mg_{1/3}Nb_{2/3})O_3$ composition, J. Mater. Res. 4 (1989) 930–944.

[17] M.-C. Chae, N.-K. Kim, J.-J. Kim, S.-H. Cho, Preparation and dielectric properties of $Pb[(Mg_{1/3}Ta_{2/3}), (Zn_{1/3}Nb_{2/3})]O_3$ relaxor ceramics, Ferroelectrics 211 (1998) 25–39.

[18] D.-H. Lee, N.-K. Kim, Crystallographic, dielectric, and diffuseness characteristics of PZN-PT ceramics, Mater. Lett. 34 (1998) 299–304.

[19] J.-S. Kim, N.-K. Kim, Lead magnesium tantalate–lead titanate perovskite ceramic system: preparation and characterization, Mater. Res. Bull. 35 (2000) 2479–2489.

[20] D.-H. Suh, D.-H. Lee, N.-K. Kim, Phase developments and dielectric/ferroelectric responses in the PMN-PT system, J. Eur. Ceram. Soc. 22 (2002) 219–223.

[21] Y. Matsuo, H. Sasaki, S. Hayakawa, F. Kanamaru, M. Koizumi, High-pressure synthesis of perovskite-type $Pb(Zn_{1/3}Nb_{2/3})O_3$, J. Am. Ceram. Soc. 52 (1969) 516–517.

[22] J. Wang, D. Wan, J. Xue, W.B. Ng, Synthesizing nanocrystalline $Pb(Zn_{1/3}Nb_{2/3})O_3$ powders from mixed oxides, J. Am. Ceram. Soc. 82 (1999) 477–479.